SOL → GEL → GLASS: I. GELATION AND GEL STRUCTURE *

C.J. BRINKER

Sandia National Laboratories, Albuquerque, New Mexico 87185, USA

G.W. SCHERER

Corning Glass Works, Corning, New York 14830, USA

The mechanisms of gel formation in silicate systems derived from metal alkoxides were reviewed. There is compelling experimental evidence proving, that under many conditions employed in silica gel preparation, the resulting polysilicate species formed prior to gelation is not a dense colloidal particle of anhydrous silica but instead a solvated polymeric chain or cluster. The skeletal gel phase which results during desiccation is, therefore, expected to be less highly crosslinked than the corresponding melted glass, and perhaps to contain additional excess free volume. It is proposed that, during gel densification, the desiccated gel will change to become more highly crosslinked while reducing its surface area and free volume. Thus, it is necessary to consider both the macroscopic physical structure and the local chemical structure of gels in order to explain the gel to glass conversion.

1. Introduction

The direct conversion of gels to dense bulk glasses without melting has recently stimulated much interest in sol–gel processing; however, to data no generally accepted model of this complete conversion process has been established. Numerous reports [1–3] have indicated that gel densification is strongly dependent on gel microstructure (or texture) and that it is essentially a sintering process, but this view ignores the significant effect gelation and aging conditions prior to desiccation have on densification kinetics [4]. The purpose of this series therefore is to relate gel densification to gel structure and ultimately to the gelation process itself. Part I of this series will establish a basis for distinguishing between so-called "polymeric gels" (generally those gels derived from metal alkoxide syntheses) and colloidal gels (prepared e.g. by destabilization of aqueous sols) and define the implications of gel structure on densification. Part II will describe densification during constant heating rate
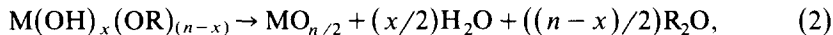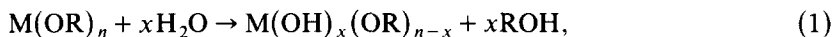
experiments and Part III will explain isothermal densification at temperatures near the T_g of the corresponding melt-prepared glass.

2. Gelation

2.1. Colloidal versus polymer gels

A gel is a form of matter intermediate between a solid and a liquid [5]. In organic systems, e.g. polyacrylamide gels, it consists of polymers or long chain molecules crosslinked to create a tangled network which extends through (thus incorporating) a liquid. The most common inorganic gel is silica gel prepared by the polymerization of monosilicic acid in aqueous solution. In contrast to organic polymers, common aqueous silica gels consist of discrete colloidal particles which are linked together into branched chains which form extensive networks throughout the liquid medium by a mechanism similar to flocculation. Interestingly, Iler states that there is no relation or analogy between silicic acid polymerized in an aqueous system and condensation type organic polymer gels [6].

The most extensively studied gels for use as glass precursors are formed by the polymerization of hydrolyzed metal alkoxides in alcoholic solutions. The net reactions to form the anhydrous oxide are generally represented as:

$$M(OR)_n + xH_2O \rightarrow M(OH)_x(OR)_{n-x} + xROH, \tag{1}$$

$$M(OH)_x(OR)_{(n-x)} \rightarrow MO_{n/2} + (x/2)H_2O + ((n-x)/2)R_2O, \tag{2}$$

In reaction (1), the water added for hydrolysis has ranged from one to over 20 mol. H_2O/mol. alkoxide [7], and the hydrolysis and condensation reactions have been catalyzed by the additions of both acids and bases. Gels have also been prepared under neutral conditions. Depending on the synthesis method, the gelation process may change significantly. In fact, one can imagine processes all the way from condensation of colloidal particles to cluster growth and crosslinking of polymeric molecules.

Partlow and Yoldas distinguished between colloidal and polymer gels in a qualitative manner especially with regard to their ability to form monolithic shapes [8]. More recently this distinction has been proven by investigations of the concentration dependence of reduced viscosity and the relationship between viscosity and molecular weight [7,9] and by small and intermediate angle X-ray scattering [10–13].

Sakka and Kamiya [7] prepared silica gels by acid (HCl) or base (NH_4OH) catalyzed hydrolysis of tetraethylorthosilicate (TEOS) with 1 to 20 mol. H_2O/mol. Si. For acid catalyzed systems prepared with 1 mol. H_2O/mol. Si,* they found a strong concentration dependence of the reduced viscosity, η_{sp}/C,

---

* Initially the molar ratio of H_2O:TEOS was 1:1, however these solutions were exposed to ambient humidity and accordingly were further hydrolyzed during the course of the experiment.

which indicates that the dissolved polymers are chain-like or linear according to the Huggins equation [13]:

$$\eta_{sp}/C = [\eta] + K[\eta]^2 C, \tag{3}$$

where η_{sp}, $[\eta]$, K, and C are the specific viscosity, the intrinsic viscosity, a proportionality constant, and the concentration of the polymer, respectively. No concentration dependence of reduced viscosity was observed for the base catalyzed system prepared with 1 mol. H_2O/mol. Si*, the acid catalyzed system prepared with 20 mol. H_2O/mol. Si, or a colloidal silica sol prepared from Ludox. This indicates that species formed in these latter systems are not linear; instead they behave like spherical particles according to the Einstein relation [14]:

$$\eta_{sp}/C = K/\rho, \tag{4}$$

where K is a constant and ρ is the particle density.

In a second study Sakka et al. [9] related the intrinsic viscosity $[\eta]$ to the number average molecular weight, M_n, by use of the following relationship [15]:

$$[\eta] = KM_n^{\alpha}, \tag{5}$$

where K is a constant and α depends on the shape of the polymers. For example α is 0.5 to 1.0 for linear polymers and close to zero for disc-shaped and spherical particles. α was found to equal 0.75 for an acid-catalyzed solution prepared with 1 mol. H_2O/mol. Si (linear polymers) while it decreased to 0.34 (highly branched clusters) for a solution prepared with 20 mol. H_2O/mol. Si. In a system prepared with an intermediate water content (5 mol. H_2O/mol. Si), α initially equaled 0.5 but decreased to 0.2 at $M_n > 10^4$, indicating that the initial chain-like polymers branch and ultimately form more highly condensed species under these conditions.

Schaefer and co-workers [10–13] used in-situ small angle X-ray scattering (SAXS) to characterize gelation in silica systems prepared with ~ 4 mol. H_2O/mol. Si using a 2-step hydrolysis procedure. The first step consisted of mixing TEOS, n-propanol, water and HCl in a molar ratio of 1 : 3 : 1 : 0.0007 at 60°C. After 90 min, additional water plus acid or base (NH_4OH) were added. (The latter sample will be referred to as "base catalyzed" even though acid was employed in the first step.) In addition to determining the size and growth kinetics of polymeric species formed during gelation by analysis of the low-angle Guinier-region of scattering, statistical information was obtained on the local structure by analysis of the intermediate-angle, (Porod) region of the scattering curve. In the Porod region, defined by the limits $KR_g \gg 1$, $Ka \ll 1$; where K is the scattering vector, R_g is the radius of gyration, and a is the size of the monomeric species; the scattered intensity is proportional to K^{-x}. The Porod exponent, x, equals 1 for a completely extended (rod-like) chain, 2 for a

random walk polymer chain or a randomly branched chain [17], and 4 for a particle with well-defined surfaces [18]. In general, for $x < 3$, the Porod exponent equals the fractal dimension of the scattering entities [19].

For silicate systems prepared using the 2-step procedure described above, x was found to equal ~ 2 for both the acid and base catalyzed silica solutions, whereas x equalled 4 for a colloidal sol prepared from LUDOX™. This showed that polymer growth did not result in colloid formation in either of the conditions studied. Instead, the species can be viewed as highly ramified macromolecules resulting from a random growth process. Small deviations from a Porod exponent of 2 were consistently observed: $x > 2$ for base systems and $x < 2$ for acid systems. This indicates that although colloidal particles are not formed, base catalyzed polymers are more highly branched or collapsed relative to ideal random linear polymers and conversely acid catalyzed polymers are less highly branched or swollen.

In addition, it should be emphasized that there was no observable change in the Porod exponent, x, at the gel point for either the acid or base systems [12,13]. This indicates that according to the Porod criterion gelation is not accompanied by phase separation in these systems. If phase separation occurs, a Porod exponent of 4 is expected as is observed in colloidal suspensions. Thus, SiO_2 gels formed under the conditions investigated by Schaefer et al. [10–13] remain single phase at the gel point and will be referred to as polymer gels in the remainder of this paper and in Parts II and III. Colloidal gels are defined as having a Porod exponent of 4.

Schaefer et al. [10–13] also investigated the concentration dependence of the correlation range obtained from the Guinier data. A strong concentration dependence was observed in the acid catalyzed solutions while no concentration dependence was observed for the base catalyzed solutions. These results indicate that polymers formed under acid catalyzed conditions are highly overlapped (entangled) prior to gelation while polymers formed under base catalyzed conditions do not interpenetrate and thus behave as discrete clusters.

The results of these two sets of experiments provide a consistent explanation of sequential polymer growth and gel formation as illustrated schematically in figs. 1 and 2 for the acid and base catalyzed systems reviewed here. Under acid catalyzed conditions and especially with low additions of water (e.g. H_2O:Si $\leqslant 5$), primarily linear or randomly branched polymers are formed which entangle and form additional branches resulting in gelation. Under basic conditions and/or with higher additions of water more highly branched clusters are formed which do not interpenetrate prior to gelation and thus behave as discrete species. In the latter case gelation occurs by the linking together of clusters in a manner similar to colloidal gel formation (depicted in fig. 3). The results of Sakka et al. [7,9] and Schaefer et al. [10–13] prove that cluster growth under basic conditions or at high water contents does not necessarily result in the formation of colloidal particles of silica as is commonly claimed.

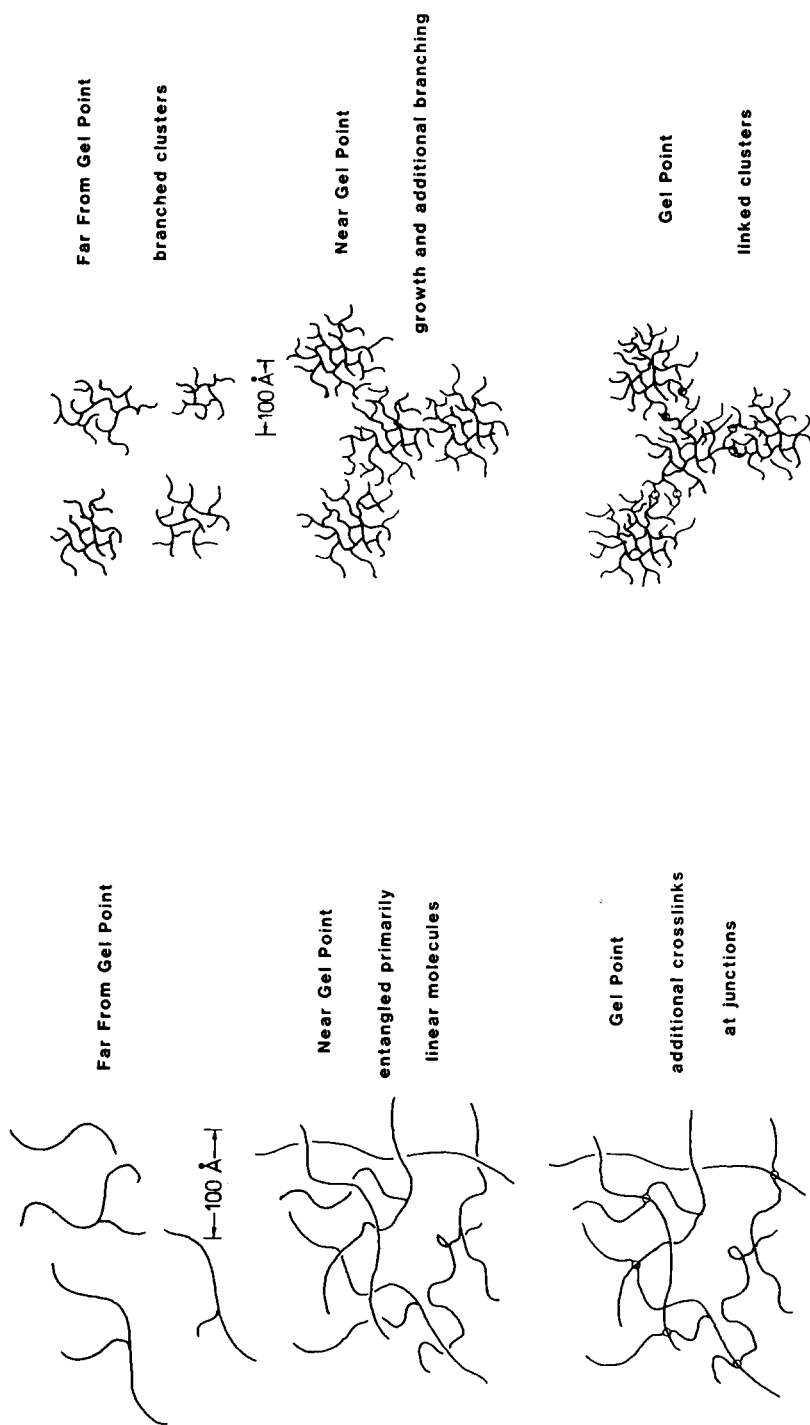Colloidal silica is formed, however, under the conditions employed by

Fig. 2. Polymer growth and gel formation in base-catalyzed systems.

Fig. 1. Polymer growth and gel formation in acid-catalyzed systems.

Stober et al. [20] In their process alkyl silicates (principally tetraethylorthosilicate) are added to basified water/alcohol mixtures. The molar ratios of H_2O:TEOS range from 7:1 to 53:1 and the total concentration of TEOS is kept low ~ 0.28M (compared to ~ 2.5M for the SAXS experiments [10–13]). Under these rather restrictive conditions, TEOS is likely to be fully hydrolyzed prior to the onset of condensation. Monosilicic acid ($Si(OH)_4$) is known to polymerize to form colloidal silica in aqueous solution as described by Iler [6]. Presumably similar growth mechanisms are operative in the mixed solvent synthesis employed by Stober et al. [20].

From consideration of the conditions which do form colloids, we may infer that more weakly crosslinked networks form when condensation commences before hydrolysis is complete [21]. ^1H NMR showed this to be the case for the 2-step hydrolysis procedure employed for the SAXS studies [12,22]. Intuition suggests that if all the monomer is quickly consumed to form dimers, trimers, etc. and possible condensation sites are limited by reducing the extent of hydrolysis, extended linear or randomly branched polymers would result (rather than dense colloids). Furthermore, it is unlikely that linkage together of these weakly crosslinked polymers could ever result in macroscopic regions of fully crosslinked oxides, since complete coalescence would be hindered sterically (e.g. interpenetration of branched polymers may be minimal). These arguments are speculative, however. A real understanding of random growth processes will only result from rigorous chemical modeling and computer simulations as being pursued by Keefer and co-workers [23].

2.2. Aging and Desiccation

Although the sharp increase in viscosity which accompanies gelation essentially freezes in a particular polymer structure at the gel point (i.e. gelation may be considered a rapid solidification process), this "frozen-in" structure may change appreciably with time (aging) depending on the temperature, solvent, and pH conditions or upon removal of solvent (desiccation). Changes in gel structure during ageing and desiccation were described by Zarzycki et al. [2] with respect to the problem of preparing monolithic gels. They described the structures of gels (prepared either by destabilization of silica sols or by

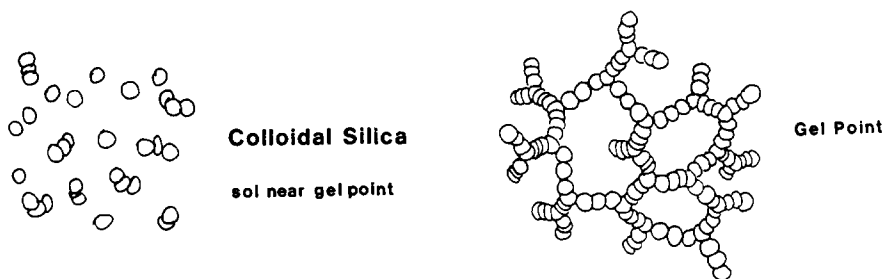**Colloidal Silica**

sol near gel point

Gel Point

Fig. 3. Colloidal gel formation.

polycondensation of organometallic compounds) according to Iler's models of aqueous silicates [6] and thus made no distinction between "polymeric" and colloidal gels. However, there is now compelling evidence that, under many conditions employed in gel preparation, single phase polymer gels rather than colloidal gels are formed. This may change the mechanisms of aging and desiccation significantly.

For example, because of the similarity in structure of certain metal alkoxide derived gels [10–12] and organic polymer gels such as polyacrylamides (both systems are composed of weakly branched polymers and are single phase at the gel point), Schaefer and Keefer recently postulated that critical phenomena such as phase separation should be observed in these inorganic systems as well [13]. According to theories established by Tanaka and others for organic polymer gels, changes in temperature, solvent quality or solvent concentration can induce phase separation (which is observed to occur reversibly in poly-acrylamide gels) [5]. Phase separation in inorganic polymer gels has not as yet been confirmed by appropriate SAXS experiments. It is expected, however, that as the critical point is approached, e.g. during a change in concentration, fluctuations in polymer density grow larger in amplitude (than those resulting merely from thermal motions) and scale as the gel separates into regions of high and low polymer density. Density fluctuations should promote additional crosslinking as unreacted terminal groups (OH and OR) come in contact in regions of higher polymer density. This increased crosslinking is expected to accelerate the phase separation process [13] and, because under most condi-tions the rate of depolymerization is low, should cause phase separation to be essentially irreversible.

Qualitative evidence in support of phase separation has been observed by Yoldas. In several reports, he shows a gel prepared from a titanium alkoxide (e.g. ref. [8]) which, under particular aging conditions, is shown to have shrunk dramatically while expelling solvent. This may represent a phase separated system gradually approaching equilibrium.

A change in chemical equilibrium may also cause phase separation. For example, if the OH^- concentration of the solvent is increased so that the rates of depolymerization and polymerization become comparable, the original gel structure will be completely transformed. Under these conditions, the most stable siloxane linkages are those involving silicon atoms bonded to four bridging oxygen atoms. As bridging oxygens are replaced with hydroxyl radicals, the remaining siloxane linkages are weakened. Thus aging at high pH will cause the gel structure to ripen. Ultimately this could result in a phase separated system composed of colloidal silica plus monosilicic acid ($Si(OH)_4$). A similar phenomenon has been observed by Bunker et al. during the aqueous corrosion of alkali silicate glasses [24].

Once liquid–solid interfaces are created, further structural changes which occur during aging can be attributed primarily to surface energy effects. It is well known that surfaces exhibiting positive radii of curvature dissolve more readily than surfaces exhibiting negative radii of curvature [6]. Therefore as the

dissolution rate is increased (e.g. by increased temperature or pH) dissolution–redeposition results in neck formation causing the gel structure to become fibrillar. Of course, when dissolution is extensive, the gel network would break down and ripen to form a colloidal sol as in the above example.

Much of the current interest in gels stems from the potential of forming monolithic pieces of glass. As a part of this process gels must be dried without cracking. Changes in gel structure during drying were described by Iler for
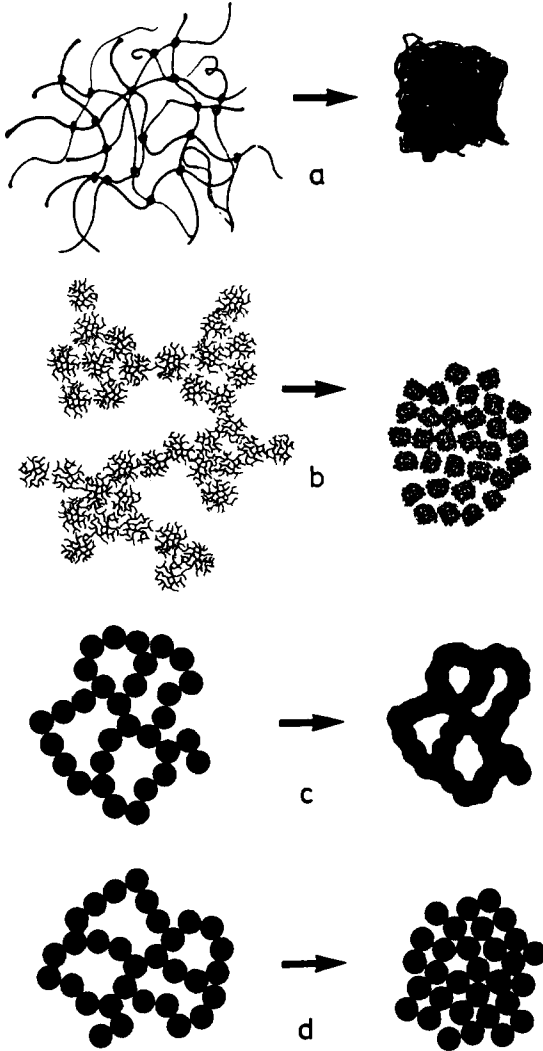

Fig. 4. Schematic representation of gel desiccation for (a) acid-catalyzed gels, (b) base-catalyzed gels, (c) colloidal gel aged under conditions of high silica solubility, (d) colloidal gel composed of weakly bonded particles.

colloidal systems [6]. According to Iler, surface tension forces created during solvent removal cause the original extended network to fold or crumple as the coordination number of the particles is increased. Porosity develops when, due to additional crosslinking or neck formation, the gel network becomes sufficiently strengthened so that it resists the compressive forces of surface tension. Thus the final desiccated gel structure (xerogel) will be a contracted and distorted version of the structure of the gel originally formed in solution (figs. 4c and d).

For polymer gels, removal of solvent is expected to collapse the network gradually resulting in additional crosslinking as unreacted hydroxyl and alkoxy groups come in contact. Depending on conditions this may induce phase separation as originally postulated by Schaefer and Keefer [13]. If so, the resulting phase separated structure may bear no relation to the structure of the gel originally formed in solution, and hence the final desiccated morphology may represent only a contracted version of this secondary phase separated structure.

If phase separation does not occur (e.g. if it is unfavorable thermodynamically or kinetically) it is expected that polymer gels will continue to collapse and crosslink until they can resist the compressive action of surface tension (at which point porosity is created). High density, low pore volume gels are therefore formed in weakly crosslinked systems when the rate of condensation is low relative to the rate of solvent removal. Under these conditions the gel structure can be highly compacted before it is sufficiently crosslinked to result in pore formation (see fig. 4a). For silica gels these conditions exist near the isoelectric point. Conversely low density gels are formed when ripening, neck growth and/or phase separation are promoted and the rate of condensation is high with respect to the rate of solvent removal. For silica gels these conditions are enhanced by increased water concentrations, intermediate pH (6–10) and elevated temperature.

There are numerous qualitative observations which support the concepts developed above. Brinker et al. prepared silica gels over a wide range of pH and water additions [11]. No microstructural features were distinguishable in the highest density xerogels ($\rho = 1.63$ g cm^{-3}) while the lowest density xerogels ($\rho = 0.68$ g cm^{-3}) prepared at pH 8.8 were distinctly globular. Since at the gel point the acid catalyzed gels were composed of entangled linear or randomly branched polymers [10–13] and the base catalyzed gels were composed of polymeric clusters [10–13]; these microstructural observations suggest that phase separation was suppressed in the acid system, whereas the globular features observed in the base system may represent the desiccated form of the original polymeric clusters or a desiccated, phase-separated structure. Nogami and Moriya observed similar microstructural features in acid and base catalyzed silica gels [1].

Brinker and Scherer prepared multi-component silicate gels with three levels each of both pH and H$_2$O additions [4]. The highest density xerogels ($\rho = 1.27$ g cm^{-3}) were obtained at pH 2.5 (near the isoelectric point of silica). Aging

these same gels for 3 weeks in 3M NH$_4$OH solution prior to desiccation restructured the gel (presumably by ripening and neck formation) causing the desiccated gel (xerogel) density to decrease to 0.72 g cm^{-3}.

3. Desiccated gel structures

It is apparent from section 2 that the physico-chemical structure of desiccated gels is a result of the complex sequence of gelation, aging, and drying conditions employed during processing. In this section we present gel structure data obtained for a borosilicate gel prepared under a particular set of gel processing conditions.

3.1. Gelation procedure

Because the ultimate goal of this investigation was to describe both the kinetics and thermodynamics of the sol → gel → glass conversion, it was necessary to prepare a gel composition which densified at sufficiently low temperatures so that both dilatometry and differential scanning calorimetry could be employed to monitor the volumetric and energetic changes which accompany densification. This temperature constraint precluded the choice of pure silica gels. Instead, a borosilicate composition, known to densify at ~ 650°C [25,26] was chosen:

66% SiO$_2$ 18% B$_2$O$_3$ 7% Al$_2$O$_3$ 6% Na$_2$O 3% BaO.

The preparation method for this gel composition is shown schematically in fig. 5 along with the pH change accompanying the sequential addition of starting compounds (measured using a Beckman Model 566471 non-aqueous pH kit). The method is basically that of Thomas [27] in which the metal alkoxides are partially hydrolyzed and added sequentially in inverse order of their corresponding rates of hydrolysis. As shown in fig. 5, the solution pH remains relatively low until the addition of sodium acetate solution. At this point, formation of the acetate–acetic acid buffer causes a rapid increase in pH. After the addition of barium acetate, the solution was cast in polypropylene test tubes and covered with aluminum foil. Gelation occurred within 24 h at room temperature. Following gelation, the covers were pierced and the gels were dried at 50°C.

The gelation conditions employed for this borosilicate composition are in a sense similar to those employed for the silica gels from which the base catalyzed gel structure model (fig. 2) was derived. However, in that study the pH was increased by addition of 1M NH$_4$OH after an initial hydrolysis step [11]. Although analogies between polymer growth (and gelation) in silicate and complex multicomponent silicate systems are questionable from a mechanistic standpoint, it is possible to infer growth structures from SAXS analyses and

PROCESSING SEQUENCE   **pH**

61.0 ml EtOH

1) 61.0 ml TEOS (Si(OC$_2$H$_5$)$_4$)   0.7

4.9 ml H$_2$O

0.2 ml 1N HCl

2) 8.8 g Al-sec-BUTOXIDE (Al(OC$_4$H$_9$)$_3$)   1.3

DISSOLVED IN 9.1 ml Iso-PrOH

3) 2.2 ml H$_2$O   1.6

17.4 ml TRIMETHYL BORATE (B(OCH$_3$)$_3$)

4) 12.9 ml H$_2$O   2.4

4.0 ml HOAc

24.6 ml 2M NaOAc

5) 12.9 ml H$_2$O   5.5

5.4 ml 1M Ba (OAc)$_2$

Fig. 5. Processing sequence for the investigated borosilicate gel. Numbers in parentheses refer to the pH measured at the corresponding stage of the gelation process.
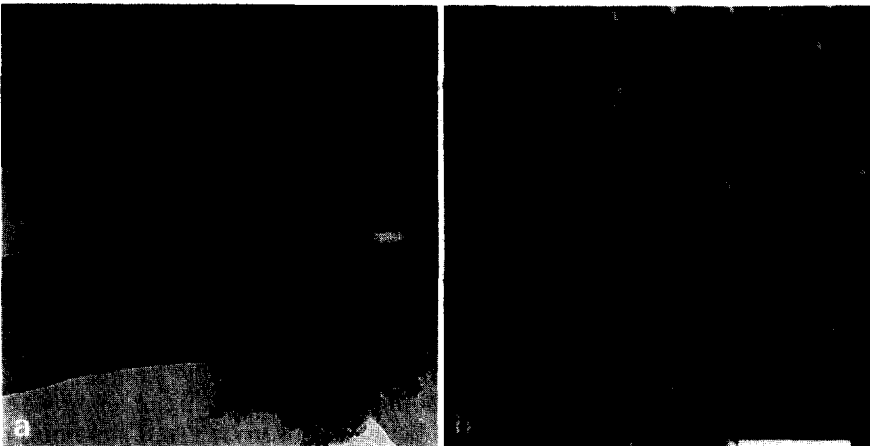

Fig. 6. (a) TEM micrograph of a gel fragment dried at 150°C and suspended on a holy carbon grid. Bar equals 50 nm. (b) SEM micrograph of a fractured surface after drying at 150°C. Bar equals 500 nm.

TEM without knowledge of the detailed chemistry. Power law analyses of SAXS results obtained for the multicomponent solution near its gel point showed that the solution consisted of macromolecular species which were weakly crosslinked compared to colloids [28]. Direct TEM of thin gel flakes desiccated at 150°C (fig. 6) revealed a necked, globular structure very similar to that of the base catalyzed gel described above [11]. These results suggest that growth in this multicomponent system results in polymeric clusters which may be topologically similar to silicate species formed under the basic conditions employed in ref. [11].

3.2. Characterization

Scanning electron microscopy (SEM), transmission electron microscopy (TEM) and nitrogen adsorption/desorption isotherm analyses were used to characterize the physical structure of the desiccated gel. For both SEM and TEM the gels were first heated to 150°C which was the degassing temperature employed for the nitrogen sorption analyses. After this heat treatment, the bulk density of the gel was measured to be 1.10 g cm^{-3} which corresponds to a relative density (ρ/ρ_s where ρ_s equals the density of the melted composition, 2.27 g cm^{-3}) of 0.48.

3.2.1. Gel microstructure

Fig. 6 shows TEM and SEM micrographs of the desiccated gel. TEM reveals that the ultrastructure consists of small globules (< 10 nm diameter) which appear to be either necked or deformed where they contact adjacent globules. It is apparent from the SEM micrograph of a fractured surface, that this globular microstructure is reproduced on a larger dimensional scale (~ 66 nm diameter). The gel was prepared under conditions in which cluster-like growth was expected (pH > 2). Therefore, the smaller globular features observed in TEM may represent either the desiccated form of the original polymeric clusters or, as discussed previously, the desiccated form of a phase separated structure. In support of this hypothesis it should be re-emphasized that globular features are not observed in silica gels prepared under conditions of low water and pH in which cluster growth and phase separation are suppressed [1,11].

Correspondingly the larger globular features observed in SEM may indicate that primary clusters agglomerate prior to gelation or that phase separation occurs on a larger dimensional scale. These secondary features also are not observed in silica gels prepared at low pH and water additions [1,11].

3.2.2. Nitrogen sorption analyses

The nitrogen adsorption–desorption isotherm is shown in fig. 7 along with pore size distributions determined from both the adsorption and desorption branches. This isotherm is a Type IV isotherm according to the classification originally proposed by Brunauer, Deming, Deming and Teller (BDDT) [29].

The characteristic feature of Type IV isotherms is the hysteresis which occurs because there are pore cavities larger in diameter than the openings (throats) leading into them (so-called ink-bottle pores). "Ink bottle" pores are expected to result from compaction of a globular or phase-separated structure during desiccation. Again it is interesting to note that adsorption–desorption isotherms obtained for silica gels prepared with low pH and H_2O contents show no hysteresis [30]. This (lack of hysteresis) is indicative of uniform-diameter microporosity [6].

In isotherms exhibiting hysteresis, the throat diameter is determined from the desorption branch while the diameter of the larger interstitial cavity is
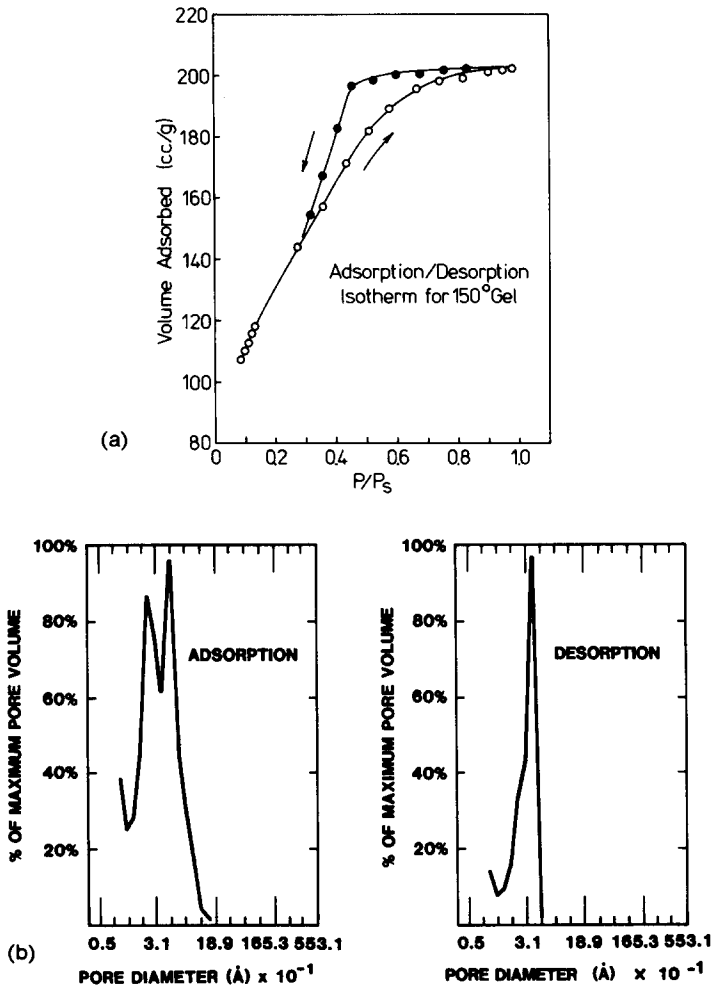

Fig. 7. (a) Adsorption-desorption isotherm of nitrogen at 77 K after vacuum degassing at 150°C for 24 h, (b) Pore size distributions determined from the adsorption and desorption branches of the isotherm shown in (a).

determined from the adsorption branch. The volume of nitrogen adsorbed near saturation, $P/P_s \sim 1$, corresponds to the total pore volume. Pore size analyses determined from the desorption and adsorption branches show a narrow distribution of small diameter pores (centered at $\sim$ 3.0 nm) and a broader distribution of larger diameter pores (centered at 4.0 nm) corresponding to the throat and interstitial cavities, respectively. Neither pore size distribution is indicative of bimodality.

3.2.3. Geometrical models

Our interest in ultimately describing gel consolidation (e.g. sintering) requires that the desiccated gel structure be modeled by a convenient geometry consistent with the measured values of surface area, pore size, and density. It should be noted that any such model will be inaccurate i.e. is inappropriate to describe statistical information in Euclidian terms; however this exercise provides some insight into possible gel structures and is necessary for subsequent analyses.

Numerous geometries have been employed to model porous solids. Most gel structure models, e.g. models of colloidal silica gels, have been based on various packing configurations of spherical particles [6]. Such models provide reasonable descriptions of the globular structures resulting from desiccation of gels consisting of clusters or phase separated structures but may be inappropriate in describing higher density xerogels which exhibit no distinguishable microstructure.

In geometrical models based on the packing of spheres, the type of packing and the sphere density determine the bulk gel density. Sphere size determines the specific surface area according to

$$Sd = 6000/\rho_{\text{skeleton}}, \tag{6}$$

where S equals surface area in $\text{m}^2 \text{ g}^{-1}$ and d equals the particle diameter in nanometers. Sphere density (or more precisely skeletal density) can be determined from the specific pore volume (V_p) by the following relation:

$$V_p = \frac{1}{\rho_{\text{gel}}} - \frac{1}{\rho_{\text{skeleton}}}, \tag{7}$$

where ρ_{gel} equals the bulk gel density and ρ_{skeleton} equals the density of the solid phase which comprises the skeletal framework. This relation assumes that there is no porosity inaccessible to N_2. Using the measured value of surface area, 496 $\text{m}^2 \text{ g}^{-1}$, in eq. (6) and the measured values of specific pore volume 0.308 $\text{cm}^3 \text{ g}^{-1}$, and bulk density, 1.10 g cm^{-3}, in eq. (7) indicates that the spheres are 7.3 nm in diameter and have a relative density of only 0.73. In order for these low density spheres to pack to a relative density of 0.48, the packing efficiency must equal 67%. This corresponds quite closely to random close packing (fig. 8) in which the average coordination number (number of particles touching each particle) equals $\sim$ 9.

This physical picture is reasonably consistent with the TEM micrograph shown in fig. 6, although the estimate of sphere size, 7.3 nm, is somewhat high

indicating that the interparticle contacts are necked or deformed [6]. According to Meissner et al. [31] the ratio of cavity radius to throat radius should equal ~ 1.4 for spheres compacted to a coordination number of 9. The measured value is closer to 1.3 which may also be indicative of neck formation. Both the measured pore size distribution and the estimated skeletal phase density dispel the notion that low bulk density is a consequence of a hierarchical microstructure (fig. 8b) in which dense particles are randomly close packed in agglomerates which are in turn randomly close packed. This microstructure would exhibit approximately the correct density, 1.02 g cm^{-3}; however, there is no evidence for the larger pores created between agglomerates (> 27.3 nm diameters for random close packing) nor is the measured skeletal density found to be that of the corresponding melted glass. This indicates that the larger globular features observed by SEM have no associated interstitial porosity (fig. 8c, d).

An alternate geometrical model which is reasonably consistent with the measured physical parameters is the cubic array shown in fig. 9. This model was developed to describe the necked, particulate SiO_2 structures formed by oxygen pyrolysis of $SiCl_4$ [33]. In this model, the cylinder diameter, $2a$, represents the average globule or cluster diameter. The bulk density of the array depends on the skeletal density and the ratio of the cylinder radius to its length, a/l. The pore diameter is related to the cube dimension, l, by equating the cross-sectional area of the pore with the area of the opening in the side of
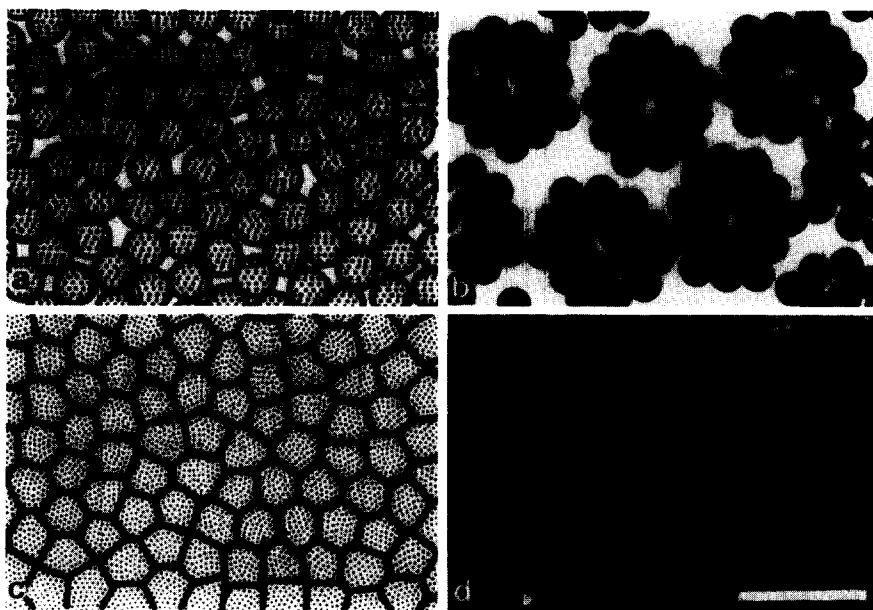

Fig. 8. (a) Random close packing of low density spheres, (b) Hierarchical random close packing of dense spheres, (c) Deformed structure representative of desiccated agglomerates (after ref. [32]) and (d) SEM micrograph of desiccated gel. Bar = 500 nm.
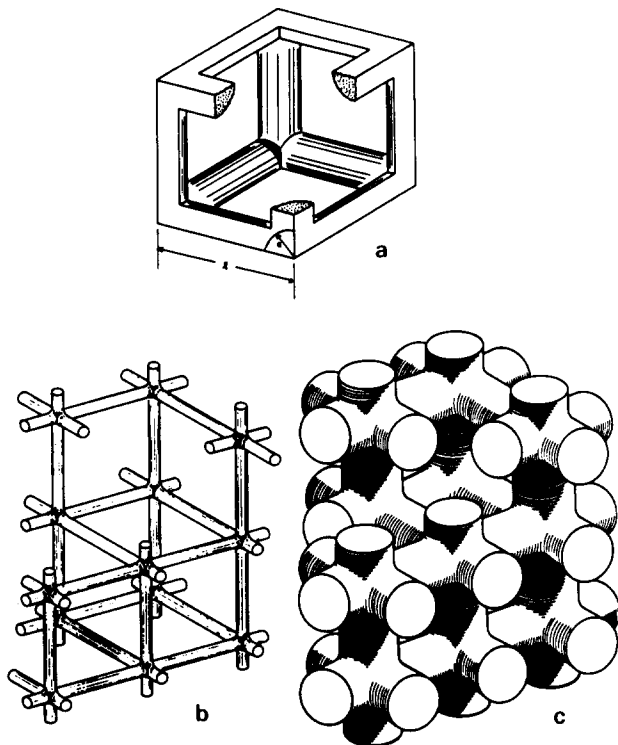
Fig. 9. (a) Cylindrical cubic array model. Dimension a is the cylinder radius and dimension l is the cell edge length, (b) fibrillar gel, (c) structure corresponding to $\rho/\rho_S = 0.48$.

the cell. Using values of bulk density and surface area measured for the borosilicate gel, and assuming the skeletal phase to be 73% dense, the cubic array model predicts a pore diameter of 1.5 nm and a cylinder diameter of 3.1 nm which are somewhat low estimates.

Analyses of the desiccated gel microstructure according to particle packing models or the cylindrical cubic array model indicate that assuming the gel to be composed of spherical particles results in an overestimate of particle diameter while assuming a cylindrical geometry results in an underestimate of the cylinder diameter. Thus, the actual xerogel microstructure can be envisioned as consisting of necked globules. The interglobule necks are not so highly developed, however, that the resulting morphology can be well described by smooth cylinders as in the cylindrical cubic array.

4. Implications of gel structure on densification

To date, the densification of gels has been treated as a sintering process in which the skeletal phase is considered to be analogous to the corresponding

melted glass. However, as pointed out in the previous sections, the gelation conditions normally employed in metal–alkoxide gel syntheses result in a wide spectrum of polymer structures ranging from weakly crosslinked polymeric chains to more highly crosslinked clusters. These structures are compacted and further polymerized during desiccation, but the resulting polymer which comprises the skeletal framework of the desiccated gel (xerogel) is likely to be less highly crosslinked than the corresponding melted glass. This provokes the following question: because the gelation process quenches in a structure which may not resemble the structure which results from a melt, how does gel structure effect gel densification? To answer this question it is necessary to consider both the thermodynamic and kinetic aspects of gel densification.

4.1. Thermodynamic aspects

Xerogels may be considered high free energy materials compared to their dense oxide counterparts prepared by melting [34]. At least three physico-chemical structural characteristics contribute to this high free energy. Surface area created by the formation of pores during desiccation makes the largest contribution, 30–300 J/g, (this corresponds to 100–1000 m^2 g^{-1} of surface area). During viscous sintering this is the energy available for viscous flow; and therefore, high surface area provides a large driving force for viscous sintering.

The remaining contributions to the high free energy of xerogels result from their reduced crosslink density compared to melted glasses. SAXS has shown that during gelation the polymeric species formed are not generally typified by dense colloidal particles but instead by more or less branched polymeric chains or clusters. Although additional polymerization occurs during desiccation, there is strong evidence that the polymeric oxide which results is less highly crosslinked than the corresponding oxide prepared by melting. For example, the number of non-bridging oxygens (OH + OR) remaining in desiccated silica gels has been estimated to range from 1.48/Si [35] to 0.33/Si [11] compared with 0.003/Si (500 ppm H_2O) for vitreous silica. This low crosslink density is one reason why the skeletal phase density of desiccated gels is less than that of the corresponding melted glass [36,37].

Because hydrolyzed silica can polymerize according to:

$$Si(OH)_4 \rightarrow SiO_2 + 2H_2O \; \Delta G_{f(298 \, K)} = -14.9 \; kJ/mol., \qquad (8)$$

more weakly crosslinked polymers (containing more non-bridging oxygen atoms) make a greater contribution to free energy than more highly crosslinked polymers. For silica gels containing 0.33 to 1.48 OH/Si, the free energy resulting from dehydration according to eq. (8) ranges from ~ 20 to 100 J/g. The free energy of formation of siloxanes is, however, very dependent on the Si–O–Si bond angle ϕ. Recent observations on silica gels suggest that dehydroxylation above ~ 300°C leads to "defective", energetic, surface species (characterized by $\phi < 150°$) which are removed only at elevated temperatures during viscous sintering [37]. Because the heat of formation of siloxane bridges

increases to + 210 kJ/mol. for cyclic disiloxanes [38] ($\phi = 87°$) the thermodynamics of the gel → glass conversion are very dependent on ϕ. This is discussed in more detail in Part II and in ref. [37].

We expect a further contribution to free energy to result from increased free volume in gels compared to melted oxides. SAXS has shown that polysilicate chains and clusters formed during gelation are weakly crosslinked (e.g. SAXS analyses indicate that acid catalyzed silicate molecules are so slightly branched that at the gel point the distance between branches is comparable to K^{-1} ($\sim$ 20 Å)[12]). It is conceivable, therefore, that on desiccation these weakly branched polymers would result in structures containing more free volume than, for example, result from a well annealed glass melt or from a colloidal gel prepared under conditions which result in a fully dense, anhydrous skeletal phase.

Free volume will reduce the skeletal density (as is observed)), but it is difficult to distinguish this effect from that of incorporation of hydroxyl groups [39] (which has the same effect on skeletal density). It is well established that excess free volume will exothermically relax at temperatures near T_g with an accompanying increase in glass viscosity [40]. Therefore, the results of Puyane et al. [41] (who observed a DTA exotherm) Brinker et al. (who observed a DSC exotherm) and Gallo et al. [42] (who observed an isothermal increase in viscosity with no accompanying dehydration) provide indirect evidence in support of excess free volume. However, direct proof of increased excess free volume in gel-derived materials awaits appropriate SAXS experiments.

Roy proposed that xerogels prepared from colloidal sols contain higher levels of structural free energy than glasses and ideal supercooled liquids [34]. Because colloidal gels are composed of an essentially anhydrous oxide skeletal phase, they contribute primarily a surface energy term to the structural free energy, i.e. they undergo little additional polymerization and contain low levels of free volume. We propose that more weakly crosslinked metal alkoxide-derived gels have even higher associated structural energies than do colloidal gels (as shown schematically in fig. 10). This distinction will be apparent in comparisons of the sintering kinetics of colloidal and "polymeric" gels [43].

4.2. Kinetic aspects

It is proposed that during the gel to glass conversion, alkoxide-derived xerogels will exothermally change to become more highly crosslinked while reducing their free volume (structural relaxation) and surface area (viscous sintering). The kinetics of this conversion are determined by both the physical and chemical structure of the desiccated gel and the time–temperature history of thermal processing. For example, condensation–polymerization, structural relaxation, and viscous sintering all depend more or less on material transport and thus are kinetically limited. Based on kinetic considerations, increased heating rates reduce the amount of time spent at each increment of tempera-

ture and, therefore, reduce the amount of viscous flow which can occur in a particular temperature interval. However, by the same argument, increased heating rates also reduce the amount of crosslinking and structural relaxation which can occur over that same interval of temperature. Because both low crosslink density [44] and excess free volume (glasses undergoing structural relaxation, i.e. those with "excess" volume, exhibit a lower activation energy for viscous flow as noted by ref. [45]) reduce the activation energy for viscous flow, increased heating rates reduce the absolute viscosity at each temperature. Therefore, it is expected that the rate of viscous sintering can actually be *increased* at sufficiently high heating rates. This is observed experimentally as described in Part II.

A second example is that of water. It is well known that water behaves as a modifier in glass in that it reduces the activation energy for viscous flow [44]. Both the amount of water and its distribution are important to the kinetics of gel densification. In colloidal gels, hydroxyl groups exist primarily on the surfaces of particles, and water content generally scales with decreasing particle size [6]. For sufficiently large particle size (reduced surface to volume ratio), gel shrinkage during heating is controlled by the viscosity of the oxide core which is essentially anhydrous. For example, there is little observed shrinkage at temperatures below T_g for colloidal silica gels consisting of ~ 50 nm diameter particles [46]. Because the oxide cores are fully crosslinked and the colloidal particles are impingent, there can be no densification without viscous flow (unless the particles rearrange themselves to a more densely packed configuration). As the particle size is reduced, the number of hydroxyl groups increases (at an equivalent surface coverage of OH), and the distribution of hydroxyl groups becomes more uniform. Ultimately (at infinitely small
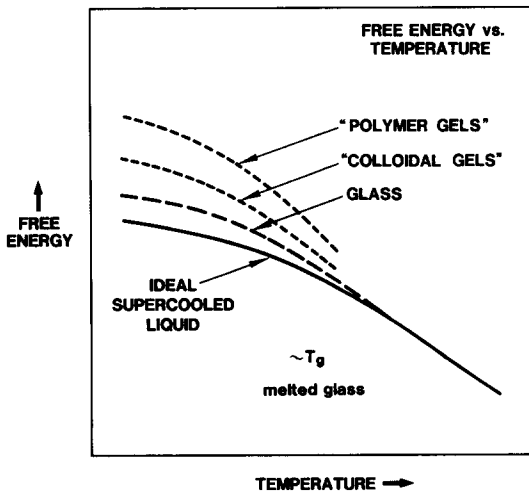

Fig. 10. Schematic representation of free energy–temperature relations between various desiccated gels, glass, and an ideal super cooled liquid of the same oxide composition.

size) there can be no distinction between surface and interior, and each silicon would have an equal probability of being bonded to a hydroxyl group. In this case, there are no large-scale regions of fully crosslinked material and on heating the structure continually evolves as polymerization (and associated shrinkage) occur continuously during the conversion to glass. This latter case (if it could be practically achieved) is quite analogous to metal alkoxide-derived-gels. SAXS results show that these systems are single phase at the gel point (Porod exponents ~ 2), and therefore there can be no distinction between surface and interior. Hydroxyl groups must be quite uniformly distributed through these single phase gels. Phase separation on drying may redistribute OH groups, but as observed by TEM the scale of phase separation (and therefore by inference the redistribution of OH) is extremely small. We believe this explains why all metal–alkoxide derived gels for which shrinkage has been measured have shrunk continuously during heating due to continued crosslinking and possibly volume relaxation. Additionally, there have been no reported measurements of T_g (by DSC or DTA) of the densifying skeleton. Although enthalpy associated with dehydroxylation, sintering, and structural relaxation might obscure the T_g endotherm, the fact that T_g has not been determined in any system may be interpreted as evidence that during the gel to glass conversion the glass structure continually evolves toward a more highly polymerized state and thus has no well-defined T_g. Only after densification (at elevated temperatures where the viscosity has been reduced to ~ 10^{13} P) do subsequent DSC measurements reveal a well-defined T_g [37].

Apart from polymer structure, xerogel microstructure also affects the kinetics of gel densification. For example, sintering models show an inverse dependence of shrinkage rate on particle size or pore size, and thus fine-textured gels are expected to densify at lower temperatures than coarse-textured gels, as is experimentally observed [1,11,46]. To date, however, gel densification has been explained primarily on the basis of microstructure alone, which ignores the often more significant effect [46] polymer structure has on gel densification.

5. Conclusions

We conclude that, based on recent experimental evidence, there is quantitative proof that polymeric species formed during gelation in metal alkoxide-derived silicate systems are generally not dense, colloidal particles but rather more or less branched polymeric chains or clusters. During desiccation these polymers are compacted and further crosslinked; however, there is evidence that the skeletal phase which comprises the desiccated gel is not identical to the corresponding melted glass. By comparison it is less highly polymerized and may contain additional free volume. Therefore, during the so-called "gel-to-glass" conversion, the desiccated gel will change to become more highly crosslinked while reducing its free volume (structural relaxation) and surface area (viscous sintering). Thus not only microstructure but also (and possibly

more importantly) local chemical structure must be considered in modeling gel densification.

References

[1] M. Nogami and Y. Moriya, J. Non-Crystalline Solids 37 (1980) 191.
[2] J. Zarzycki, M. Prassas and J. Phalippou, J. Mat. Sci. 17 (1982) 3371.
[3] J. Phalippou, M. Prassas and J. Zarzycki, Verre Refract. 35 (1981).
[4] C.J. Brinker and G.W. Scherer, Ultrastructure Processing of Glasses, Ceramics, and Composites (Wiley, New York, 1984) p. 43.
[5] T. Tanaka, Sci. Amer. (1981) 124.
[6] R.K. Iler, The Chemistry of Silica (Wiley, New York, 1979).
[7] S. Sakka and K. Kamiya, J. Non-Crystalline Solids 48 (1982) 31.
[8] D.P. Partlow and B.E. Yoldas, J. Non-Crystalline Solids 46 (1981) 153.
[9] S. Sakka, K. Kamiya, K. Makita and Y. Yamamoto, J. Non-Crystalline Solids 63 (1984) 223.
[10] D.W. Schaefer, K.D. Keefer and C.J. Brinker, Polymer Preprints, Am. Chem. Soc., Div. of Polymer Chem. 24 (1983) 239.
[11] C.J. Brinker, K.D. Keefer, D.W. Schaefer and C.S. Ashley, J. Non-Crystalline Solids 48 (1982) 47.
[12] C.J. Brinker, K.D. Keefer, D.W. Schaefer, R.A. Assink, B.D. Kay and C.S. Ashley, J. Non-Crystalline Solids 63 (1984) 45.
[13] D.W. Schaefer and K.D. Keefer, in: Better Ceramics Through Chemistry, eds., C.J. Brinker, D.E. Clark and D.A. Ulrich (North-Holland, New York, 1984) p. 1.
[14] M.L. Huggins, J. Am. Chem. Soc. 64 (1942) 2716.
[15] A. Einstein, Ann. Phys. 19 (1906) 289; 34 (1911) 591.
[16] W.J. Badgley and H. Mark, High Molecular Weight Organic Compounds, eds., R.E. Burk and O. Grummitt (Interscience, New York, 1949) p. 75.
[17] D. Stauffer, A. Coniglio and M. Adams, Advances in Polymer Science, 44 (Springer, Berlin, 1982).
[18] G. Porod, Kolloid Z. 124 (1951) 83.
[19] T.A. Witten and L.M. Sander, Phys. Rev. Lett. 47 (1981) 1400.
[20] W. Stober, A. Fink, and E. Bohn, J. Colloid Interface Sci. 26 (1968) 62.
[21] K.D. Keefer, in: Better Ceramics Through Chemistry, eds., C.J. Brinker, D.E. Clark and D.R. Ulrich (North-Holland, New York, 1984) p. 15.
[22] R.A. Assink and B.D. Kay, in: Better Ceramics Through Chemistry, eds., C.J. Brinker, D.E. Clark and D.R. Ulrich (North-Holland, New York, 1984) p. 301.
[23] K.D. Keefer, to be published.
[24] B.C. Bunker, T.J. Headley and S.C. Douglas, in: Better Ceramics Through Chemistry, eds., C.J. Brinker, D.E. Clark and D.R. Ulrich (North-Holland, New York, 1984) p. 41.
[25] C.J. Brinker and S.P. Mukherjee, J. Mat. Sci. 16 (1981) 1980.
[26] C.J. Brinker and S.P. Mukherjee, Thin Solid Films 77 (1981) 141.
[27] I.M. Thomas, US Patent No. 3 799 754 (1974).
[28] K.D. Keefer and C.J. Brinker, unpublished results.
[29] S. Brunauer, L.S. Demig, W.S. Deming and E. Teller, J. Am. Chem. Soc. 62 (1940) 1723.
[30] D.M. Krol and J.G. van Lierop, J. Non-Crystalline Solids 63 (1984) 131.

[31] H.P. Meissner, A.S. Michaels and R. Kaiser, Ind. Eng. Chem. Process Des. Div. 3 (1964) 202.

[32] A.C. Wright, G.A.N. Cornell and J.W. Allen, J. Non-Crystalline Solids 42 (1980) 69.

[33] G.W. Scherer, J. Am. Ceram. Soc. 60 (1977) 236.

[34] R. Roy, J. Am. Ceram. Soc. 52 (1969) 344.

[35] M. Yamane, S. Aso, S. Okano and T. Sakaino, J. Mat. Sci. 14 (1979) 607.

[36] N. Tohge, G.S. Moore and J.D. Mackenzie, J. Non-Crystalline Solids 63 (1984) 95.

[37] C.J. Brinker, E.P. Roth, G.W. Scherer and D.R. Tallant, J. Non-Crystalline Solids, to be published.

[38] A.G. Revesz and G.V. Gibbs, in: the Physics of MOS Insulators, eds., G. Lucovsky, S.T. Pantelides and F.L. Galeener (Pergamon, New York, 1980).

[39] J. Acocella, M. Tomozawa and E.B. Watson, J. Non-Crystalline Solids 65 (1984) 355.

[40] S.M. Rekhson et al., Sov. J. Inorganic Materials 7 (1971) 622.

[41] R. Puyane, P.F. James and H. Rawson, J. Non-Crystalline Solids 41 (1980) 105.

[42] T.A. Gallo, C.J. Brinker, L.C. Klein and G.W. Scherer, in: Better Ceramics Through Chemistry, eds., C.J. Brinker, D.E. Clark, D.R. Ulrich (North-Holland, New York, 1984). p. 85.

[43] G.W. Scherer and C.J. Brinker, Sol Gel Glass III, J. Non-Crystalline Solids, to be published.

[44] G. Hetherington, K.H. Jack and J.C. Kennedy, Phys. Chem. Glasses 5 (1964) 130.

[45] O.S. Narayanaswamy, J. Am. Ceram. Soc. 54 (1971) 491.

[46] C.J. Brinker, W.D. Drotning and G.W. Scherer, in: Better Ceramics Through Chemistry, eds., C.J. Brinker, D.E. Clark, and D.R. Ulrich (North-Holland, New York, 1984) p. 25.